Assessing the protective role of active agriculture on wildfire exposure in a Mediterranean region

Marcos Rodrigues[1,2,*], Carmen Bentué[1,3], Minia Blanco[1], Isabel Gómez-Lain[1], Marcelo Ramos[1], Paloma Ibarra[1,2]

[1] Department of Geography and Land Management, C/Pedro Cerbuna 12, 50009, Zaragoza (Spain)

[2] GEOFOREST Research group, University Institute for Environmental Sciences

[3] GEOT Research group, University Institute for Environmental Sciences

*Corresponding author: rmarcos@unizar.es

Abstract

Global change and rural abandonment are restructuring Mediterranean fire regimes, as landscapes once characterized by heterogeneous agricultural mosaics are progressively replaced by homogenized, drought-limited fuel complexes. This transformation increases the likelihood of high-intensity wildfire events and their associated impacts. This study applied a stochastic fire-spread modeling framework based on thousands of simulated wildfire events to quantify the effects of land abandonment in the Matarranya region in eastern Spain, comparing current landscape conditions with a counterfactual "no-abandonment" scenario. Results indicate that active agriculture serves as a critical passive infrastructure protection system by maintaining fuel discontinuity, yielding a 75% mean reduction in building exposure ($\beta = 0.24$). Conversely, land abandonment functions as an exposure multiplier, triggering a 7-fold increase in the number of structures reaching high and very high burn probability threshold. Abandonment also raises burning intensity (flame length), which limits suppression capability. Overall, the cessation of management roughly tripled potential fire size and quadrupled exposure of human infrastructure, highlighting the importance of identifying "high-leverage plots" where targeted agricultural restoration maximizes safety. By strategically prioritizing these parcels, planners can transform abandoned land into revenue-generating firebreaks and functional strategic fire zones (SFZs), establishing an evidence-based framework for rural development and wildfire risk mitigation.

Keywords: wildfire risk assessment, land abandonment, stochastic modeling, infrastructure exposure, Mediterranean landscape

1. Introduction

Global change is restructuring the relationship between terrestrial ecosystems and wildfire regimes (Bowman et al., 2009; Seidl et al., 2011, 2017). Rising temperatures and prolonged droughts have extended the fire season (Jolly et al., 2015), while the structural connectivity of the landscape has increased the severity and intensity of these events (Erdozain et al., 2024). In Mediterranean Europe, landscape homogenization into horizontally and vertically continuous fuel arrangements is a key factor modulating the potential for extreme wildfires. This configuration reflects a shift from fuel-limited to drought-driven wildfire regimes (Pausas & Fernández-Muñoz, 2012). Recent megafire episodes across Europe illustrate this escalation (European Commission. Joint Research Centre et al., 2025; Linley et al., 2025). In 2025 alone, EFFIS (European Forest Fire Information System) reported more than 1,000,000 ha burned, nearly three times the 2006–2024 average. This trend marks a departure from traditional "cultural fire regimes," in which primary land-use activities limited fuel continuity, leading to a new paradigm characterized by unprecedented fire extremes (Seijo & Gray, 2012).

Over the past decades, the Mediterranean basin has experienced a profound landscape transformation, largely driven by widespread agricultural land abandonment (Estel et al., 2015; Lasanta et al., 2017). The cessation of traditional land-use practices has triggered a "forest transition," marked by the encroachment of woody vegetation into formerly heterogeneous agricultural mosaics (Vidal-Macua et al., 2018). In Spain, this process is generally associated with cessation of agricultural activity and lack of proactive forest management, particularly in mountainous areas (Ameztegui et al., 2016). Evidence indicates that fire activity may intensify where silvicultural interventions are restricted under certain forms of environmental protection (Resco De Dios, Cunill Camprubí, et al., 2025; Resco De Dios, Schütze, et al., 2025). The loss of the traditional landscape mosaic has significantly raised the likelihood of high-intensity wildfire events (Viedma et al., 2015), compounded by increasing fuel aridity (Chaparro et al., 2016; Rodrigues, Camprubí, et al., 2023). Despite these trends, the consequences of forest transition remain insufficiently characterized, especially at the local scale (Schulp et al., 2019), where finegrained landscape structure governs fire spread and behavior (Finney, 2002; Finney et al., 2011).

In response to this escalating risk, the EU Civil Protection Mechanism emphasizes the need for readiness and anticipatory planning to face destructive wildfire seasons (European Parliament and Council of the European Union, 2021). Robust risk assessment and public awareness are essential for adapting to emerging fire regimes (Moreira et al., 2020; Wunder et al., 2021), providing a necessary framework for effective risk mitigation strategies (Cochrane & Bowman, 2021). Contemporary wildfire management prioritizes quantitative risk assessment grounded in probabilistic representation of exposure—particularly burn probability (BP)—over descriptive approaches (Ager et al., 2021; Alcasena, Ager, et al., 2021; Alcasena et al., 2022; Palaiologou et al., 2026; Parisien et al., 2019; Salis et al., 2018). Stochastic fire-spread modeling is fundamental in this context, as it captures the inherent variability of fire occurrence by simulating numerous potential scenarios. These methodologies move beyond "worst-case" planning and instead identify the underlying landscape configurations that govern fire spread (Finney, 2005; Parisien et al., 2019).

Accordingly, this study applied a stochastic fire-spread modeling framework integrating spatially explicit fire-occurrence patterns with historical fire weather distributions to quantify burn probability—reflecting exposure levels—and flame length—representing potential burn intensity. This probabilistic approach is particularly suited to exploring scenarios that reflect the range of potential fire situations. The analysis focused on the Matarranya region, located in the Spanish province (NUTS3) of Teruel. Matarranya has experienced substantial agricultural abandonment, mirroring broader rural trends across Aragon and Spain. Historically, the region has recorded recurrent high-intensity fires from both natural and anthropogenic sources (Amatulli et al., 2007).

The primary objective of this study was to present a methodology to evaluate the effects of land abandonment on fire risk transmission and landscape-scale exposure (Ager et al., 2017). Thousands of plausible wildfire events were simulated under two distinct landscape configurations: the current landscape condition and a counterfactual scenario in which abandoned plots remained functional. A comparative analysis of these landscape states was conducted to evaluate changes in the spatial distribution of BP, risk transmission hotspots, and infrastructure exposure. The analysis establishes a baseline for estimating changes in expected fire frequency and return intervals,(RI), offering a replicable methodology for decision making in other regions. The main contribution of this work is the comprehensive integration of multiple aspects of stochastic modeling for exposure assessment. Empirical ignition models—incorporating both human and natural drivers—were coupled with suppression capabilities to determine location of fire initiation. While existing assessments are often based on historical evidence of abandonment, this approach relies on the actual spatial footprint of rewilding (Bachantourian et al., 2023; Salis et al., 2022). Furthermore, the study incorporates annualized outputs in the identification of priority intervention areas, a feature frequently absent when optimization is the primary objective (Carrasco-Barra et al., 2025). Simulations were calibrated to reproduce observed fire weather conditions and fire-size distributions, improving representation of the prevailing fire regime. When combined with land-abandonment data, this methodology assesses changes in exposure and risk transmission and improves the communication of results to planners and decision makers. The approach aligns with Strategic Environmental Assessment requirements (Granceri Bradaschia et al., 2024; Ledda et al., 2021) by providing a framework that evaluates potential wildfire impacts while explicitly characterizing the baseline conditions (current abandonment), interventions (agricultural plot recovery), and derived effects (change in exposure, intensity and risk transmission).

2. Methodology

2.1. Study Area

The study was conducted in the Matarranya region, province of Teruel, in northeastern Spain (Autonomous Community of Aragon; Figure 1). The *comarca* covers approximately 933 km² and comprises 18 municipalities with a total population of 8,267 inhabitants (INE, 2024), resulting in a population density of less than 10 inhabitants per km². Matarranya represents a characteristic Mediterranean landscape marked by pronounced territorial and environmental contrasts. The region has experienced sustained depopulation and agricultural land abandonment, with approximately 3,338 ha abandoned between 1984 and 2009 (Rich & Ibarra, 2015). These trends contributed to the degradation of cultural and agrarian landscapes. Historically, Matarranya has been defined by a characteristic mosaic of dry-stone wall terraces and flat-bottomed valleys ("*vales*"), which generated marked structural diversity across the landscape. The cessation of cropping and livestock farming led to widespread woody encroachment, as former olive and almond groves were replaced by dense scrublands and spontaneous woody vegetation. This homogenization of the landscape matrix increased fuel loads and transformed the environment from a fragmented mosaic to a forest continuum (Rich & Ibarra, 2015).

The relief reflects the convergence of the Iberian System and the Catalan Coastal Ranges. The terrain exhibits a complex orography characterized by a pronounced altitudinal gradient, ranging from 300 masl in the northern agricultural plains to nearly 1,400 masl in the southern mountains. The climate is Mediterranean with continental influences. Mean annual precipitation varies from approximately 400 mm in the northern plains to over 700 mm in the southern highlands. Land cover consists of a mosaic of traditional dryland crops (olive, almond, vineyards) and expanding stands of *Pinus halepensis* and *Quercus ilex*, the latter largely associated with terrace abandonment since the mid-20th century.

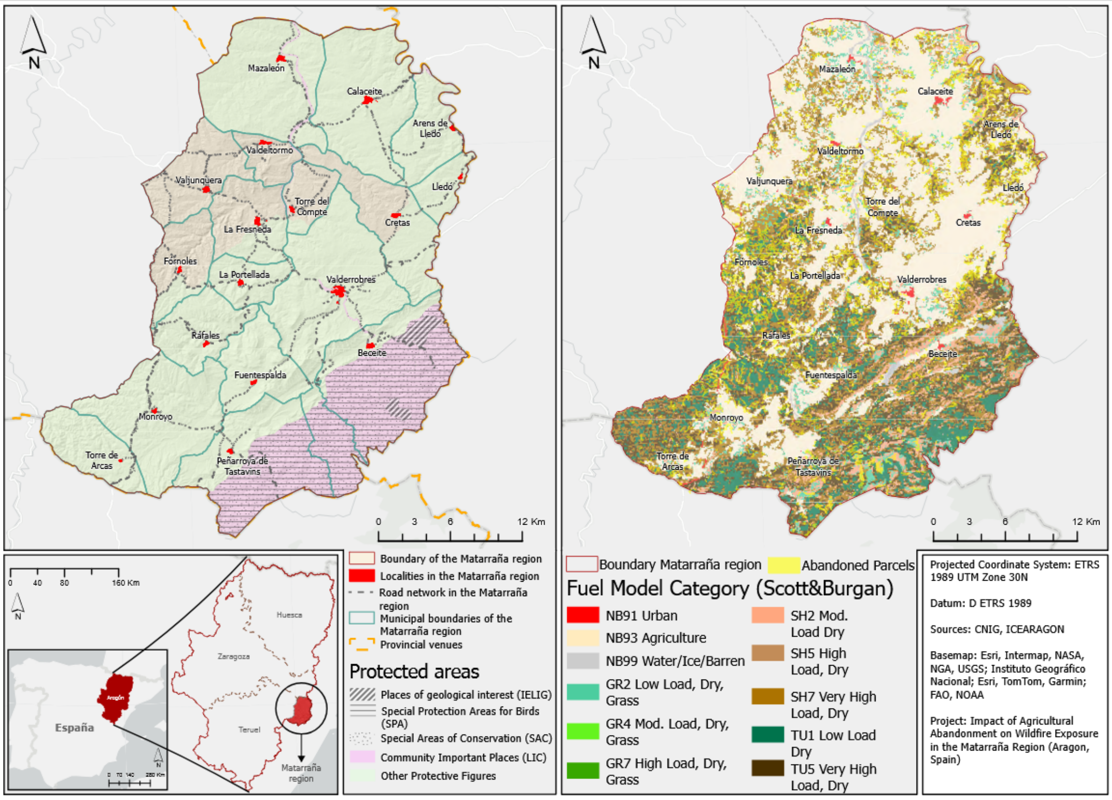

Figure 1. Study area: Matarranya region (Aragon, Spain). Location of the study area in northeastern Spain, including municipal boundaries and main settlements.

2.2. Datasets for stochastic fire spread and behavior

2.2.1. Location of abandoned plots

Abandoned croplands were obtained from the Matarranya Land Bank cartography (Rich & Ibarra, 2015). This dataset integrates photointerpretation of orthophotographs (PNOA 2009, 0.5 m resolution; regional flight 2008, 0.25 m resolution) with historical aerial imagery from 1984 (IGN, 1:30,000 scale) to delineate abandoned agricultural parcels. Pre-1984 abandonment was identified through comparison with 1956 aerial photography (https://pnoa.ign.es/pnoa-imagen/vuelos-y-ortofotos-historicas). The analysis was further refined by consulting land-use data such as CORINE Land Cover maps (European Environment Agency, 2019a, 2019b) and the Spanish Forest Map (Ministerio de Medio Ambiente, 1997). The final product is a vector polygon layer in which each feature corresponds to an abandoned plot.

2.2.2. Fire-occurrence probability

Fire-occurrence probability (P_o) defines the spatial allocation of ignition seeds used in the spread simulation algorithm (Parisien et al., 2019). In this study, P_o was the likelihood that an ignition—natural or anthropogenic—develops into a spreading fire exceeding 10 ha and escapes initial suppression efforts (Arienti et al., 2006), thus representing extreme wildfire conditions (Alcasena et al., 2022). P_o was calculated from multiple products available in the study area. Human-caused ignition likelihood (P_h) was estimated following Gelabert et al. (2025) and implemented as described in Rodrigues and Gelabert (2025a); lightning-caused ignition (P_l) was calculated according to Rodrigues et al. (2023b) and implemented as described in Rodrigues and Gelabert (2025b); and probability of escape from initial attack (P_e) was determined following Rodrigues et al. (2019) and implemented as described in Rodrigues and Gelabert Vadillo (2025c). All datasets were provided at 200 × 200 m resolution. Operationally, P_o was calculated as follows:

$$P_o = (P_h \cap P_l) \cup P_e$$

where P_h denotes anthropogenic ignition probability, P_l natural ignition probability, and P_e the probability of escape from initial attack.

The region exhibits a higher proportion of lightning-caused fires (Amatulli et al., 2007), compared with other Mediterranean environments, where fires are predominantly anthropogenic (San-Miguel-Ayanz et al., 2012). The intersection of ignition probability ($P_h \cap P_l$) was calculated using a weighting scheme, with P_h representing 80% and P_l 20%.

2.2.3. Landscape data for spread simulation

Fire behavior simulations require spatial layers characterizing topography (elevation, slope, aspect), surface fuel models (Scott & Burgan, 2005), and canopy attributes (height, cover, bulk density, base height), collectively forming the landscape file. These inputs were obtained from the pan-European fuel map server (Kutchartt et al., 2024), which provides raster layers at 100 × 100 m resolution, with all the necessary information to conduct the simulations. To introduce the effect of land abandonment, the surface fuel layer was modified by reclassifying abandoned plots as non-burnable (NB) (fuel model code 93; Scott & Burgan, 2005). Pixels in the original fuel map whose centroids fell within abandoned plot polygons were reassigned accordingly. Two landscape files were therefore generated, one for each surface fuel scenario.

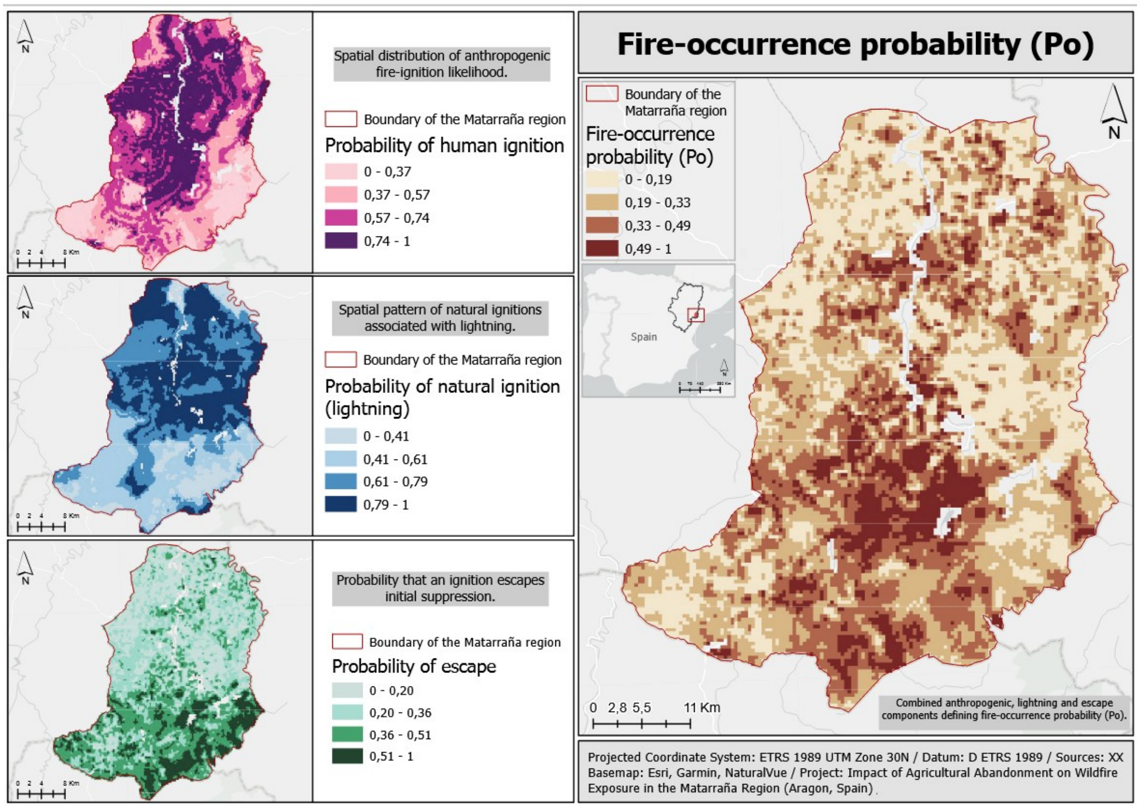

Figure 2. Spatial distribution of fire-occurrence probability. Left panels show individual ignition probabilities and escaping fires. The right panel shows the P_o used to assemble simulated perimeters into BP_a.

2.3. Stochastic wildfire spread simulation and burn probability estimates

Fire propagation was simulated using the FConstMTT command-line application (Missoula Fire Sciences Laboratory, 2024), implementing a core version of the minimum travel time algorithm (MTT; Finney, 2002). Simulations were conducted under two scenarios: the current situation with abandoned croplands (AB), and a counterfactual scenario in which all parcels retained active woody crops and were therefore non-burnable (NO_AB). A total of 20,676 wildfire events were simulated under extreme fire weather conditions (5th percentile dead fuel moisture content, 95th percentile wind speed, and 90–60% live woody-herbaceous moisture content). Simulations were proportionally distributed across four synoptic weather patterns derived from observed wildfires in the region (Table S1). Ignition seeds were allocated based on P_o (Figure 2). Following common practice, simulations were calibrated to reproduce historical fire-size distributions (Parisien et al., 2019), following Rodrigues (2025). The ensemble of simulations represents the equivalent of 10,000 fire seasons—sufficient to affect all burnable pixels at least once. Annual burn probability (BP_a) was then calculated for each 100 ×100 m grid cell within the study area as:

$$BP_a = \frac{N_p}{n}$$

where N_p is the number of simulated fire perimeters intersecting grid cell p, and n is the total number of simulated seasons. Individual BP_a surfaces were generated for each land-use scenario to allow spatial comparison of wildfire exposure under changing agricultural conditions.

Simulations were replicated under the NO_AB scenario using the alternative fuel layer that restores agricultural practices in AB parcels. By maintaining identical ignition seeds and weather conditions, a second BP_a map was generated and subsequently compared with the baseline AB scenario.

2.4. Exposure assessment

Wildfire exposure was defined as the probability that a given infrastructure element or asset is affected by fire as a function of burning intensity. Building infrastructure exposure was analyzed by functional use (urban, industrial, or agricultural). Building footprints were obtained from the Spanish National Topographic Base (BTN; IGN, 2018) and later converted into centroid points for further analysis. Building features were assigned a functional use based on SIOSE (Land Cover / Land Use Information System of Spain) high-resolution dataset (IGN, 2022), which classifies land parcels based on the HILUCS

(Hierarchical INSPIRE Land Use Classification System). Each building polygon from the BTN dataset was spatially overlaid with the SIOSE land-use layer, and the dominant HILUCS code within each footprint was extracted and reclassified into one of three functional categories.

Exposure was quantified by combining building presence and BP_a values at each location. In the first step, infrastructures exposed in each BP_a class were determined, using breaks at 0.0010, 0.0020, 0.0034, and 0.0067, which defined five classes corresponding to fire RI of 1000, 500, 300, and 150 years. A second exposure metric estimated the annual average infrastructure loss by multiplying the total number of buildings by their respective BP_a values. This yielded an aggregated value representing the expected annual number of buildings affected by fires. Finally, to characterize the potential burning intensity, flame-length values from the spread simulations were extracted for all locations with non-zero BP_a. Four ordinal exposure classes were defined using the recommended Byram's fireline intensity (<1.2, 1.2–3.4, and >3.4 m) by the National Wildfire Coordinating Group (2006).

2.5. Risk transmission

Risk transmission represents the potential of the landscape to affect exposed assets. It is based on identifying clusters or hotspots from which fires that may affect a given resource originate (Ager et al., 2017). From the ensemble of simulated events, fires intersecting buildings were extracted and their ignition points retrieved. Each ignition location was assigned a weight corresponding to the number of buildings potentially affected. Using these weighted ignition points, kernel density estimates (KDE) were generated for both scenarios using a fixed bandwidth of 400 m and a resolution of 25 x 25 m. The resulting KDE raster surfaces represent the spatial footprint of ignition pressure on infrastructure. KDE densities were reclassified into five ordinal classes ("very low" to "very high") based on upper quantile thresholds (P75 to P99) calculated across both scenarios.

2.6. Statistical analysis

The AB and NO_AB scenarios were compared using linear regression analysis, modeling the relationship between BPs at the building level under both scenarios. R^2 coefficient and the β regression coefficients were extracted for each structure to evaluate slopes against the identity line (AB = NO_AB). At the plot level, total burned area of perimeters intersecting each plot was compared with the total number of exposed buildings. These analyses provided the basis for parameterizing changes in exposure and determining the capacity of specific plots to disrupt fire propagation. This approach yields a systematic ranking of plots based on their priority for restoration and recovery.

3. Results

3.1. Spatial patterns and change in annual burn probability

Of the 20,676 fires simulated under the AB baseline, 4,098 originated within abandoned plots, reducing the number of effective perimeters assembled into BP_a to 16,578. The simulations reproduced the historical distribution with sufficient fidelity, showing a 6% difference in observed density (Figure S1).

Land abandonment substantially increased BP_a in the region, thereby shortening the expected fire RI (Figure 3 and Figure S2). High BP_a clusters were concentrated near Valjunquera in the mid-western sector, and near Monroyo and Penyarolla de Tastavins in the south. Under the NO_AB scenario, most of the territory fell within the “very low” BP interval class (≤ 0.001 or >1000y RI), while only a few isolated patches in the south-eastern sector—near settlements such as Beceite, Fuentespalda, and Peñarroya de Tastavins—reached medium (≤ 0.003) or high (≤ 0.004) values. The mean BP_a under AB was 0.001, approximately twice the 0.00049 observed under NO_AB. Areas with fire RI below 300 years exhibited a notable reduction. Overall, the absence of abandonment extended the mean RI by 843 years, increasing the expected return period from 800 to 1,498 years.

3.2. Exposure to wildfires

3.2.1. Exposed buildings

Under NO_AB conditions, the number of exposed buildings decreased by 26.4%, from 3,254 in the current AB scenario to 2,396 (Table *1*). Under NO_AB, the expected annual average of burned buildings declined from 4.35 to 1.69. Nearly eight out of ten structures (80.1%) were located in NB areas, and 11.3% fell within the “very low” class (< 0.001), leaving 8.6% above this threshold. Reversing agricultural abandonment increased the proportion of buildings in NB areas by 5.2%, while all non-zero probability classes above the “very low” interval contracted. The 0.001–0.002 class decreased from 567 to 292 buildings, and the 0.002–0.0033 class from 466 to 186. High-end exposure was largely confined to the AB scenario. Buildings in the “high” (0.003–0.004) and “very high”

(> 0.004) classes were seven times more exposed under AB, with 366 buildings compared to 51 under NO_AB.

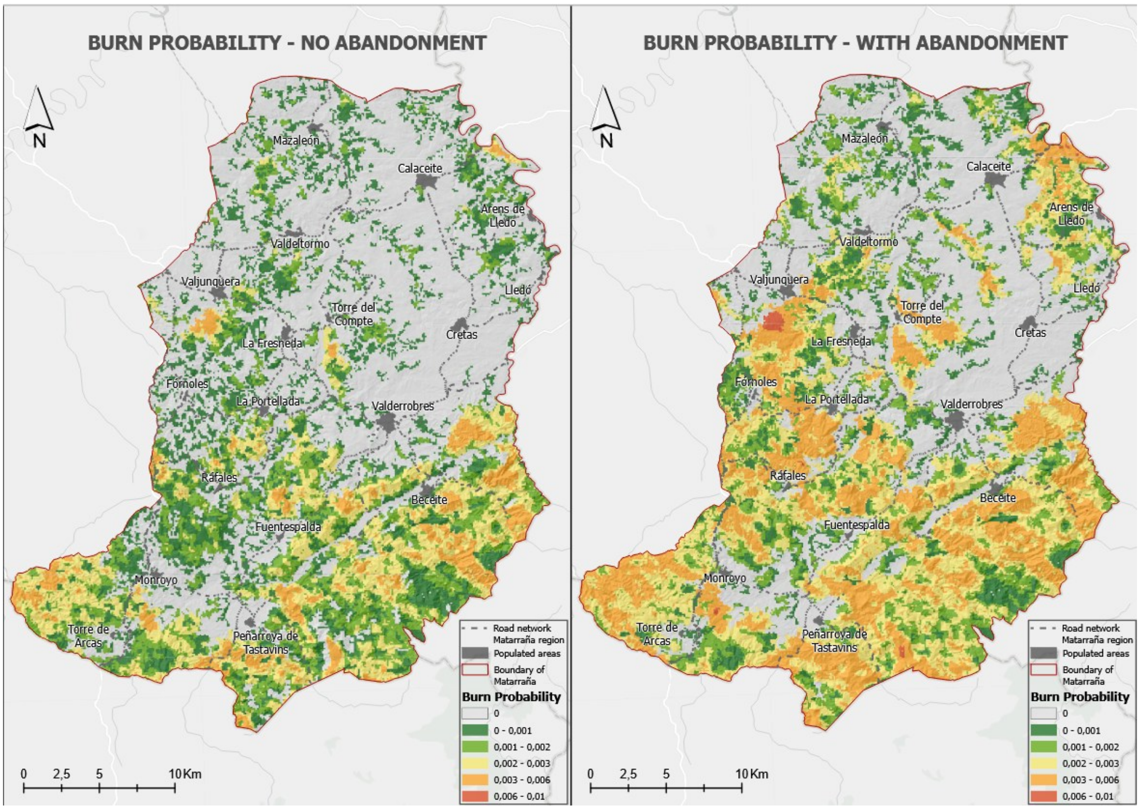

Figure 3. Spatial distribution of BP_a across the Matarranya region under two land-use scenarios: (left) no-abandonment (NO_AB), (right) abandonment (AB). Burn probability (BP) classes are expressed as return intervals (RI) with breakpoints at 0.0010, 0.0020, 0.0033, 0.0066 BP_a, corresponding to 1000, 500, 300 and 150 years.

Table 1. Distribution of buildings by BP_a class under abandonment (AB) and no-abandonment (NO_AB) scenarios. n is the number of buildings, pct the percentage of buildings and N_BP is the average annual number of fire-affected buildings.

BPa	AB_n	AB_pct	N_BP_AB	NOAB_n	NOAB_pct	N_BP_NOAB
NB	13,068	80.1	-	13,926	85.3	-
0–0.001	1,850	11.3	0.74	1,867	11.4	0.60
0.001–0.002	567	3.5	0.84	292	1.8	0.42
0.002–0.0033	466	2.9	1.22	186	1.1	0.48
0.0033–0.0066	366	2.2	1.52	51	0.3	0.20
>0.0066	5	0.03	0.04	0	0.0	0.00
	3,254		4.35	2,396		1.69

3.2.2. Exposure by functional land use

The comparative analysis of building-scale BP_a revealed systematically higher wildfire exposure across all functional land-use categories under AB conditions. As illustrated in Figure 4, the distribution consistently fell below the identity line, indicating universally higher BP_a following land abandonment. Linear regression models fitted to each functional class showed a high degree of correlation, with relatively high R^2 coefficients, indicating that the spatial pattern of risk was largely preserved but shifted toward higher probability magnitudes. However, regression lines diverge substantially from the identity line, particularly at higher probability thresholds. Slope regression coefficients of approximately 0.4 correspond to a 2.5-fold increase in BP_a.

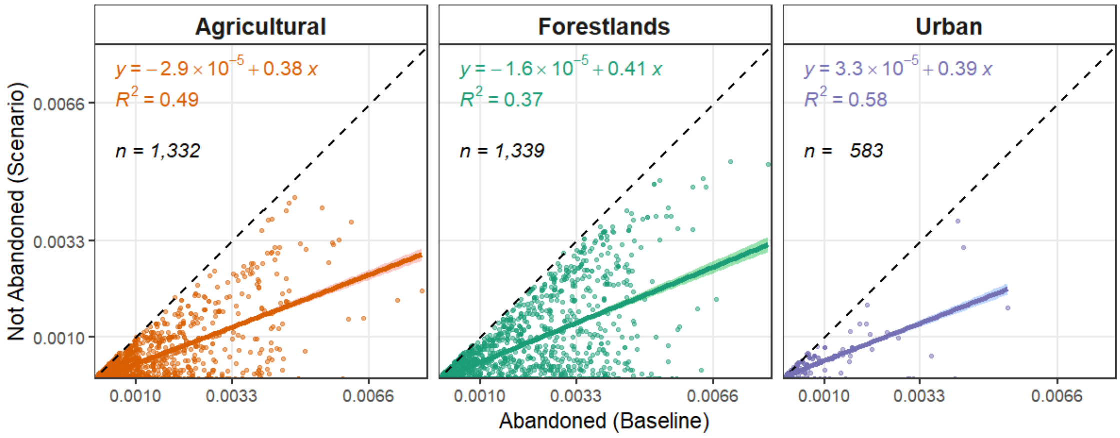

Figure 4. Building-scale comparison of BP between the abandonment (AB) baseline and the no-abandonment (NO_AB) scenario by functional land use. The dashed line represents the perfect identity line, while colored lines show the fitted linear regression between BP_a with and without abandonment, including the equation and R^2 coefficient. Each point represents a building, with n standing for the total number of buildings per category.

3.2.3. Burning intensity in terms of flame length

1. The comparative analysis of fire behavior revealed a marked increase in potential fire intensity across the Matarranya region under the two situations (Figure 5 and Figure S3). NO_AB conditions preserved a heterogeneous mosaic, with active agricultural plots maintaining extensive swathes of low-intensity fuels (green, <1.2 m). Under AB, this heterogeneity was lost due to landscape homogenization. “High” (yellow, 2.4–3.4 m) and “extreme” (red, > 3.4 m) flame-length classes expanded as former croplands were colonized by scrublands and forest fuels. This expansion created a continuous, high-load fuel matrix in which fires propagated with greater energy, particularly where extreme-intensity classes (> 3.4 m) encroached upon populated areas such as Valderrobres and Beceite. Regarding building exposure, all flame-length classes affected fewer structures under the NO_AB scenario (. Spatial distribution of flame-length (FL) across the Matarranya region under two land-use scenarios: (left) no-abandonment (NO_AB), (right)

abandonment (AB). FL classes were defined according to fireline intensity thresholds from the National Wildfire Coordinating Group (2006).

Table *2*). The largest reductions occurred in intervals exceeding 2.4 m: approximately 6% of buildings were affected by high/extreme fire behavior under AB, compared with 3.5% under NO_AB. The second-largest change occurred in the NB class, in which 5% of buildings were no longer exposed to fire. Moderate and low-intensity fire behavior showed limited variation.

3.3. Plot influence in propagation and exposure

The assessment of plot influence revealed a significant increase in fire impact under AB across both evaluated metrics. All data points fell below the identity line, confirming that restoring plots reduced fire exposure. For total burned area (left), the regression slope (0.33) indicated that, on average, the NO_AB scenario lowered simulated fire size by approximately 67%. The model explained a moderate proportion of variance ($R^2 = 0.49$), suggesting that the impact varied with the surrounding landscape configuration. A comparable pattern was observed for building exposure (right panel). The regression slope (0.24; $R^2 = 0.49$) showed a stronger proportional reduction in affected buildings than in fire size, with the AB scenario reaching roughly 75% more buildings. Spatial analysis of plot influence identified several distinct core clusters of highly influential locations. For fire-size reduction (Figure S4), one major cluster appeared in the mid-west region and two secondary clusters in the north-east and south-west. For building exposure, a principal cluster was located in the mid-west sector, with a secondary cluster in the south-east. The mid-west region emerged as the most influential area across both metrics.

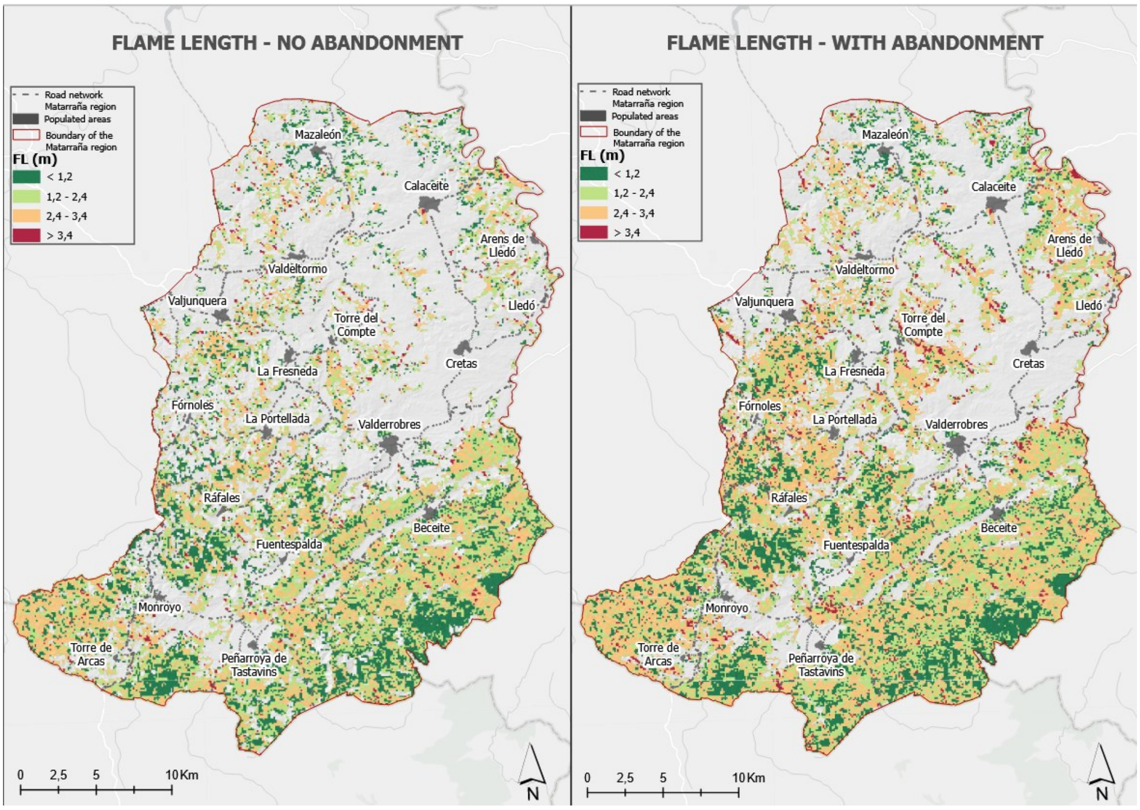

Figure 5. Spatial distribution of flame-length (FL) across the Matarranya region under two land-use scenarios: (left) no-abandonment (NO_AB), (right) abandonment (AB). FL classes were defined according to fireline intensity thresholds from the National Wildfire Coordinating Group (2006).

Table 2. Number and percentage of buildings with burn probability > 0 in each flame-length (FL) class under abandonment (AB) and no-abandonment (NO_AB) scenarios.

FL (m)	AB	AB%	NO_AB	NO_AB%	Fireline intensity	Tactical recommendations (National Wildfire Coordinating Group, 2006)
NB	13,255	81.2	14,037	86.0	-	-
≤1.2	834	5.1	690	4.2	Low	Direct attack by hand crews is usually successful
1.2–2.4	1257	7.7	1,024	6.3	Moderate	Too intense for hand tools
2.4–3.4	818	5.0	476	2.9	High	Control efforts at the head will likely fail
>3.4	158	1.0	95	0.6	Extreme	Direct attack is dangerous and ineffective

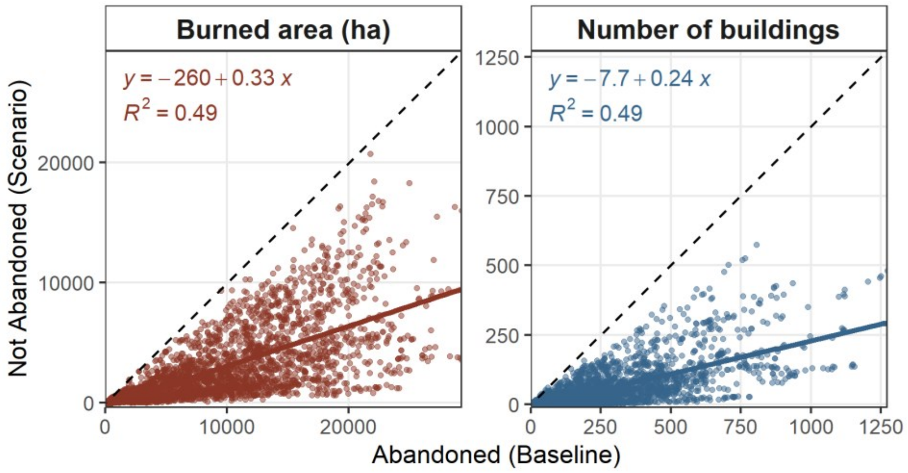

Figure 6. Comparison of total fire size (left) and number of exposed buildings (right) at plot scale between the abandonment (AB) baseline and the no-abandonment (NO_AB) scenario. The dashed line represents the identity line; colored lines show the fitted linear regression, including the regression equation and R^2 coefficient. Each point represents a plot.

3.4. Transmission risk into building

The spatial distribution of fire transmission risk—defined as the density of ignition points likely to propagate and impact structural assets—exhibited a marked shift between the two land-use scenarios (Figure 7). Under AB, KDE identified extensive and contiguous "very high" risk clusters forming a consolidated north–south corridor through the central sector, particularly around the municipalities of Fórnoles, La Portellada, and Ráfales. In contrast, under NO_AB, this spatial connectivity was disrupted, and former large-scale hotspots fragmented into isolated and less intense patches. Regression analysis supported this spatial contraction, indicating a 75% mean reduction in exposed buildings when agricultural plots were restored ($\beta = 0.24$, $R^2 = 0.49$; Figure 6). These results demonstrate that active land maintenance functions as a critical spatial intervention that prevents fire propagation toward infrastructure in high-vulnerability areas such as Beceite and Peñarroya de Tastavins.

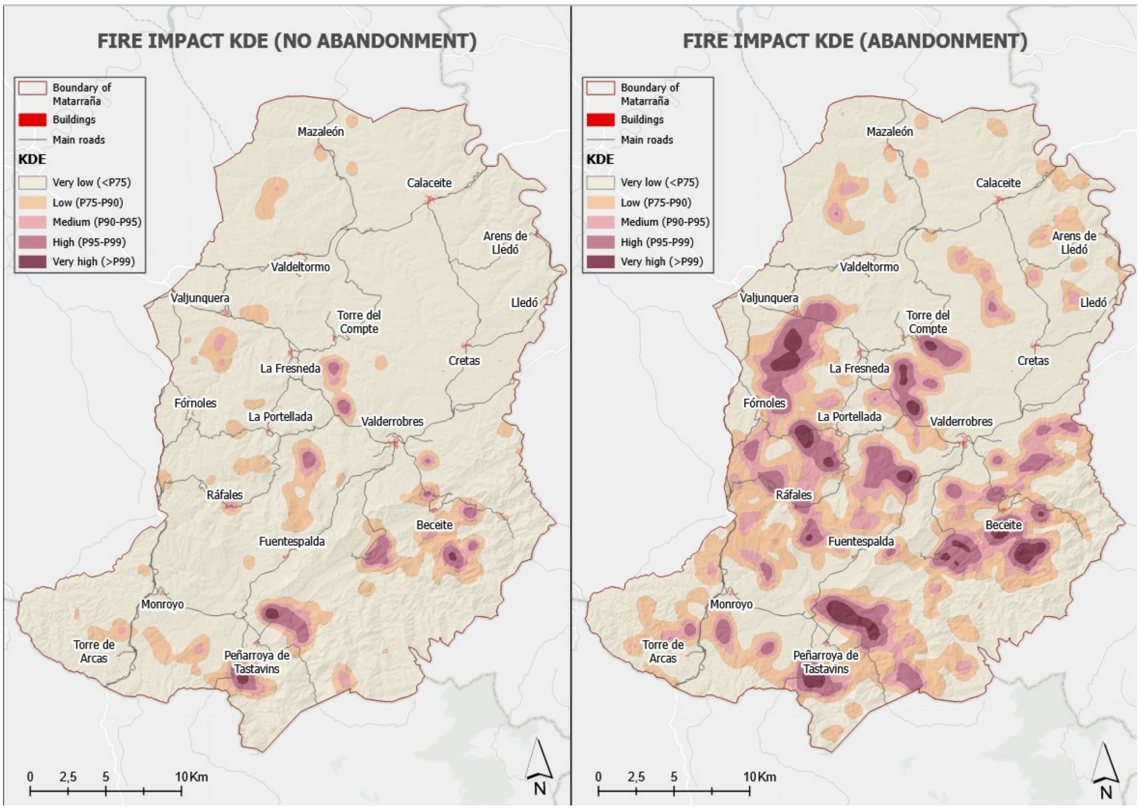

Figure 7. Spatial distribution of density of buildings calculated using Kernel Density Estimation (KDE) across the Matarranya region under two land-use scenarios: (left) no-abandonment (NO_AB) and (right) abandonment (AB).

4. Discussion

This study integrates empirical inputs (ignition and suppression potential) with stochastic modeling (wildfire spread simulation) to quantify the effects of land abandonment in a representative Mediterranean landscape in eastern Spain. This approach establishes a baseline for assessing landscape-level wildfire exposure and infrastructure vulnerability, and identifies critical hotspots where highly threatening fire events are most likely to originate.

4.1. Influence of land abandonment on landscape homogenization and spread potential

The findings highlight the role of active agriculture in maintaining a heterogeneous mosaic that disrupts fuel continuity (Moreira et al., 2011). Under NO_AB, a 5.2% increase in non-burnable areas, together with fragmentation of extreme-risk patches in the southwestern highlands, illustrates how agricultural activity functions as a passive protective mechanism for infrastructure. Reversing rewilding creates heterogeneity in the landscape, which limits fire propagation by effectively re-fragmenting fuel beds and protecting the building stock by preventing the critical connectivity required for large fires (Bertomeu et al., 2022; Ursino & Romano, 2014). Within this context, maintaining agricultural activity extends beyond socio-economic considerations, serving as a strategy to counteract rewilding processes (Sil et al., 2024). The 7-fold increase in buildings exposed to "high" and "very high" probability thresholds (BP from 0.003 to > 0.004; Figure 3) indicates that land abandonment acts as an exposure multiplier (Salis et al., 2022). The marked divergence from the identity line (slope coefficients around 0.4; Figure 4) reveals a systematic intensification of exposure. This "tail risk" is particularly relevant for the 8.6% of the building stock exceeding the highest probability threshold. Overall, under land abandonment structures enter an extreme-exposure category that would otherwise remain uncommon under active agricultural management (Alcasena et al., 2017; Lasanta et al., 2022; Salis et al., 2018).

4.2. Intensification of fire behavior and related implications

Differences in flame-length distributions (Figure 5) provide evidence that abandonment increases burn intensity and constrains suppression effectiveness. Expansion of the 1.2–2.4 m and 2.4–3.4 m classes along the central valley corridor suggests that under current AB conditions operational thresholds have been exceeded. In these sectors, manual suppression is becomes ineffective requiring indirect strategies, heavy machinery, or aerial support, which increases costs (Stougiannidou & Zafeiriou, 2022). This transition complicates fire-fighting logistics and increases the likelihood that small ignitions develop into large-scale events that exceed the control capacity of local emergency services. Nearly 1,000 buildings fall within high-risk categories under AB (FL > 2.4 m), compared with approximately 570 under managed conditions. The avoided cost of fire damage may offset the subsidies required to keep marginal land in production (Simon et al., 2022), positioning agricultural maintenance as a modern, cost-effective infrastructure protection strategy (Lecina-Diaz et al., 2023). By maintaining 90.2% of structures within the NB or "very low" exposure classes (Table 2), the region preserves its socio-economic core while avoiding areas of "high" and "very high" exposure.

4.3. Plot-scale mitigation and links with decision making

Extending the analysis from landscape-level observations to building-scale BP_a provides a more precise and management-oriented perspective. The cessation of agricultural management nearly triples potential burned area and quadruples building exposure (Figure 6). Plots differ markedly in their influence on exposure and transmission risk, and these differences shift between land-use states (Figure S4), revealing strategic positions for risk mitigation. Identifying these specific parcels allows for a prioritized restoration strategy (Rich & Ibarra, 2015). Rather than pursuing full regional reversal of abandonment—which is unlikely—planners can concentrate efforts on "high-leverage plots," where reintroducing agricultural activity yields the greatest reduction in building exposure per hectare. Targeted recovery of abandoned plots contributes to the formation of a "functional mosaic" that functions as a persistent firebreak while maintaining economic revenue. The use of plot-scale data to prioritize these zones directs limited rural-development resources toward areas delivering the highest safety return for both built stock and the emergency responders responsible for its defense (Alcasena, Rodrigues, et al., 2021). Evaluating the "mitigation yield" of reverting individual plots to a non-burnable state offers an empirical basis for defining and ranking strategic fire zones (SFZs). Under this framework, SFZs evolve from mere administrative boundaries into functional landscape units defined by their risk-reduction potential (North et al., 2024). Critical mitigation zones were identified with clusters of managed plots forming a defensible buffer. Final prioritization on interventions, however, requires further refinement of approaches (Carrasco-Barra et al., 2025).

5. Conclusions and final remarks

Land abandonment in Mediterranean regions represents not only a socio-economic transition but also a key driver of environmental hazard intensification, highlighting the need for a paradigm shift in wildfire risk assessment. By applying a stochastic modeling framework to isolate the effects of agricultural cessation, this study demonstrates that active land management functions as a critical system for infrastructure protection. The progression from landscape-scale observations to plot-level prioritization offers a scalable methodology for moving from broad administrative directives to functional Strategic Environmental Assessment. Recognizing the mitigation potential of agricultural restoration improves resource allocation and transforms the environmental challenge of rewilding into an opportunity for proactive, evidence-based wildfire mitigation strategy.

Funding

This work was financed by the projects FireCycle (CNS2023-144228) funded by the Spanish Ministry of Science and Innovation (MCIN/AEI/10.13039/501100011033) and project “Understanding Wildfire Risk: A Local-Scale Assessment Framework in Chile”, financed by the AXA Research Fund. The work has been also supported by project FLARE (PID2023-148568OB-I00).

Acknowledgements

We would like to give special thanks to the Matarranya Land Bank for sharing the dataset of abandoned plots, which was essential for developing this work.

References

Ager, A. A., Day, M. A., Alcasena, F. J., Evers, C. R., Short, K. C., & Grenfell, I. (2021). Predicting Paradise: Modeling future wildfire disasters in the western US. *Science of The Total Environment*, *784*, 147057. https://doi.org/10.1016/j.scitotenv.2021.147057

Ager, A. A., Evers, C. R., Day, M. A., Preisler, H. K., Barros, A. M. G., & Nielsen-Pincus, M. (2017). Network analysis of wildfire transmission and implications for risk governance. *PLOS ONE*, *12*(3), 1-28. https://doi.org/10.1371/journal.pone.0172867

Alcasena, F., Ager, A., Le Page, Y., Bessa, P., Loureiro, C., & Oliveira, T. (2021). Assessing Wildfire Exposure to Communities and Protected Areas in Portugal. *Fire*, *4*(4), 82. https://doi.org/10.3390/fire4040082

Alcasena, F. J., Salis, M., Ager, A. A., Castell, R., & Vega-García, C. (2017). Assessing Wildland Fire Risk Transmission to Communities in Northern Spain. *Forests*, *8*(2). https://doi.org/10.3390/f8020030

Alcasena, F., Rodrigues, M., Gelabert, P., Ager, A., Salis, M., Ameztegui, A., Cervera, T., & Vega-García, C. (2021). Fostering carbon credits to finance wildfire risk reduction forest management in mediterranean landscapes. *Land*, *10*(10). https://doi.org/10.3390/land10101104

Alcasena, F., Rodrigues, M., Gelabert, P., & Vega-García, C. (2022). Advancing New Methods for Creating Fire-Resilient Communities in Mediterranean Areas. *Environmental Sciences Proceedings*, *17*(1). https://doi.org/10.3390/environsciproc2022017070

Amatulli, G., Peréz-Cabello, F., & de la Riva, J. (2007). Mapping lightning/human-caused wildfires occurrence under ignition point location uncertainty. *Ecological Modelling*, *200*(3–4), 321-333. https://doi.org/10.1016/j.ecolmodel.2006.08.001

Ameztegui, A., Coll, L., Brotons, L., & Ninot, J. M. (2016). Land-use legacies rather than climate change are driving the recent upward shift of the mountain tree line in the Pyrenees: Past human use drives upward tree line shift in the Pyrenees. *Global Ecology and Biogeography*, *25*(3), 263-273. https://doi.org/10.1111/geb.12407

Arienti, M. C., Cumming, S. G., & Boutin, S. (2006). Empirical models of forest fire initial attack success probabilities: The effects of fuels, anthropogenic linear features, fire weather, and management. *Canadian Journal of Forest Research*, *36*(12), 3155-3166. https://doi.org/10.1139/x06-188

Bachantourian, M., Kalabokidis, K., Palaiologou, P., & Chaleplis, K. (2023). Optimizing Fuel Treatments Allocation to Protect the Wildland–Urban Interface from Large-Scale Wildfires in Greece. *Fire*, *6*(2), 75. https://doi.org/10.3390/fire6020075

Bertomeu, M., Pineda, J., & Pulido, F. (2022). Managing Wildfire Risk in Mosaic Landscapes: A Case Study of the Upper Gata River Catchment in Sierra de Gata, Spain. *Land*, *11*(4), 465. https://doi.org/10.3390/land11040465

Bowman, D. M. J. S., Bowman, D. M. J. S., Balch, J. K., Artaxo, P., Bond, W. J., Carlson, J. M., Cochrane, M. A., Antonio, C. M. D., Defries, R. S., Doyle, J. C., Harrison, S. P., Johnston, F. H., Keeley, J. E., & Krawchuk, M. A. (2009). Fire in the Earth System. *Science*, *481*(April), 481-484. https://doi.org/10.1126/science.1163886

Carrasco-Barra, J., Gonzalez-Olabarria, J. R., Palacios, D., Mahaluf, R., Garcia-Gonzalo, J., & Weintraub, A. (2025). Multicriteria firebreak planning for protecting ecological and cultural values under Wildfire risk: A case study in Catalonia. *Environmental and Sustainability Indicators*, *28*, 100956. https://doi.org/10.1016/j.indic.2025.100956

Chaparro, D., Piles, M., Vall-llossera, M., & Camps, A. (2016). Surface moisture and temperature trends anticipate drought conditions linked to wildfire activity in the Iberian Peninsula. *European Journal of Remote Sensing*, *49*(1), 955-971. https://doi.org/10.5721/EuJRS20164950

Cochrane, M. A., & Bowman, D. M. J. S. (2021). Manage fire regimes, not fires. *Nature Geoscience*, *14*(7), 455-457. https://doi.org/10.1038/s41561-021-00791-4

Erdozain, M., Alberdi, I., Aszalós, R., Bollmann, K., Detsis, V., Diaci, J., Đodan, M., Efthimiou, G., Gálhidy, L., Haase, M., Hoffmann, J., Jaymond, D., Johann, E., Jørgensen, H., Krumm, F., Kuuluvainen, T., Lachat, T., Lapin, K., Lindner, M., … de-Miguel, S. (2024). The Evolution of Forest Restoration in Europe: A Synthesis for a Step Forward Based on National Expert Knowledge. *Current Forestry Reports*, *11*(1), 4. https://doi.org/10.1007/s40725-024-00235-3

Estel, S., Kuemmerle, T., Alcántara, C., Levers, C., Prishchepov, A., & Hostert, P. (2015). Mapping farmland abandonment and recultivation across Europe using MODIS NDVI time series. *Remote Sensing of Environment*, *163*, 312-325. https://doi.org/10.1016/j.rse.2015.03.028

European Commission. Joint Research Centre, Sedano, F., San-Miguel-Ayanz, J., Broglia, M., Durrant, T., Boca, R., Maianti, P., Oom, D., Branco, A., Rigo, D. de, Suarez-Moreno, M., Ferrari, D., Roglia, E., Scionti, N., Libertà, G., & Tistan, A. (2025). *Forest fires in Europe, Middle East and North Africa 2024*. Publications Office of the European Union. https://data.europa.eu/doi/10.2760/0649290

European Environment Agency. (2019a). *CORINE Land Cover 1990 (vector), Europe, 6-yearly—Version 2020_20u1, May 2020* (Versión 20.01) [FGeo,Spatialite]. European Environment Agency. https://doi.org/10.2909/5C1F2E03-FCBA-47B1-AFEB-BC05A47BADA0

European Environment Agency. (2019b). *CORINE Land Cover 2000 (vector), Europe, 6-yearly—Version 2020_20u1, May 2020* (Versión 20.01) [FGeo,Spatialite]. European Environment Agency. https://doi.org/10.2909/8B85B479-6AFB-42C6-817C-11D1A5260B83

European Parliament and Council of the European Union. (2021). *Regulation (EU) 2021/836 of the European Parliament and of the Council of 20 May 2021 amending Decision No 1313/2013/EU on a Union Civil Protection Mechanism*. https://eur-lex.europa.eu/eli/reg/2021/836/oj

Finney, M. A. (2002). Fire growth using minimum travel time methods. *Canadian Journal of Forest Research*, *32*(8), 1420-1424. https://doi.org/10.1139/x02-068

Finney, M. A. (2005). The challenge of quantitative risk analysis for wildland fire. *Forest Ecology and Management*, *211*(1–2), 97-108. https://doi.org/10.1016/j.foreco.2005.02.010

Finney, M. A., McHugh, C. W., Grenfell, I. C., Riley, K. L., & Short, K. C. (2011). A simulation of probabilistic wildfire risk components for the continental United States. *Stochastic Environmental Research and Risk Assessment*, *25*(7), 973-1000. https://doi.org/10.1007/s00477-011-0462-z

Gelabert, P., Jiménez-Ruano, A., Ribalaygua, J., Torres, L., & Rodrigues, M. (2025). Human-caused ignition pathways under climate change scenarios in Eastern Spain. *Geomatics, Natural Hazards and Risk*, *16*(1), 2472864. https://doi.org/10.1080/19475705.2025.2472864

Granceri Bradaschia, M., Longato, D., Maragno, D., & Musco, F. (2024). Climate change adaptation mainstreaming through strategic environmental assessments. An in-depth analysis of environmental indicators from spatial plans in Friuli Venezia Giulia Region (Italy). *Environmental Impact Assessment Review*, *109*, 107650. https://doi.org/10.1016/j.eiar.2024.107650

IGN. (2018). *Mapas vectoriales y bases cartográficas y topográficas a escala 1:25,000 para explotación y consulta mediante sistemas de información geográfica.* Instituto Geográfico Nacional, Ministerio de Fomento. https://www.ign.es/web/ign/portal

IGN. (2022). *Sistema de Información sobre Ocupación del Suelo de España (SIOSE)*. Ministerio de Transportes, Movilidad y Agenda Urbana.

Jolly, W. M., Cochrane, M. a, Freeborn, P. H., Holden, Z. a, Brown, T. J., Williamson, G. J., & Bowman, D. M. J. S. (2015). Climate-induced variations in global wildfire danger from 1979 to 2013. *Nature communications*, *6*(May), 7537. https://doi.org/10.1038/ncomms8537

Kutchartt, E., González-Olabarria, J. R., Aquilué, N., Garcia-Gonzalo, J., Trasobares, A., Botequim, B., Hauglin, M., Palaiologou, P., Vassilev, V., Cardil, A., Navarrete, M. Á., Orazio, C., & Pirotti, F. (2024). Pan-European fuel map server: An open-geodata portal for supporting fire risk assessment. *Geomatica*, *76*(2), 100036. https://doi.org/10.1016/j.geomat.2024.100036

Lasanta, T., Arnáez, J., Pascual, N., Ruiz-Flaño, P., Errea, M. P., & Lana-Renault, N. (2017). Space–time process and drivers of land abandonment in Europe. *Catena*, *149*, 810-823. https://doi.org/10.1016/j.catena.2016.02.024

Lasanta, T., Cortijos-López, M., Errea, M. P., Khorchani, M., & Nadal-Romero, E. (2022). An environmental management experience to control wildfires in the mid-mountain mediterranean area: Shrub clearing to generate mosaic landscapes. *Land Use Policy*, *118*, 106147. https://doi.org/10.1016/j.landusepol.2022.106147

Lecina-Diaz, J., Chas-Amil, M.-L., Aquilué, N., Sil, Â., Brotons, L., Regos, A., & Touza, J. (2023). Incorporating fire-smartness into agricultural policies reduces suppression costs and ecosystem services damages from wildfires. *Journal of Environmental Management*, *337*, 117707. https://doi.org/10.1016/j.jenvman.2023.117707

Ledda, A., Di Cesare, E. A., Satta, G., Cocco, G., & De Montis, A. (2021). Integrating adaptation to climate change in regional plans and programmes: The role of strategic environmental assessment. *Environmental Impact Assessment Review*, *91*, 106655. https://doi.org/10.1016/j.eiar.2021.106655

Linley, G. D., Jolly, C. J., Doherty, T. S., Geary, W. L., Armenteras, D., Belcher, C. M., Bliege Bird, R., Duane, A., Fletcher, M., Giorgis, M. A., Haslem, A., Jones, G. M., Kelly, L. T., Lee, C. K. F., Nolan, R. H., Parr, C. L., Pausas, J. G., Price, J. N., Regos, A., … Nimmo, D. G. (2025). 'Megafire'—You May Not Like It, But You Cannot Avoid It. *Global Ecology and Biogeography*, *34*(4), e70032. https://doi.org/10.1111/geb.70032

Ministerio de Medio Ambiente. (1997). *Mapa Forestal de España a escala 1:200000*.

Missoula Fire Sciences Laboratory. (2024). *Command Line Applications for Fire Behavior and First Order Fire Effects Calculations*. https://www.firelab.org/ (or specific software URL if available)

Moreira, F., Ascoli, D., Safford, H., Adams, M. A., Moreno, J. M., Pereira, J. M. C., Catry, F. X., Armesto, J., Bond, W., González, M. E., Curt, T., Koutsias, N., McCaw, L., Price, O., Pausas, J. G., Rigolot, E., Stephens, S., Tavsanoglu, C., Vallejo, V. R., … Fernandes, P. M. (2020). Wildfire management in Mediterranean-type regions: Paradigm change needed. *Environmental Research Letters*, *15*(1), 011001. https://doi.org/10.1088/1748-9326/ab541e

Moreira, F., Viedma, O., Arianoutsou, M., Curt, T., Koutsias, N., Rigolot, E., Barbati, A., Corona, P., Vaz, P., Xanthopoulos, G., Mouillot, F., & Bilgili, E. (2011). Landscape—Wildfire interactions in southern Europe: Implications for landscape management. *Journal of Environmental Management*, *92*(10), 2389-2402. https://doi.org/10.1016/j.jenvman.2011.06.028

National Wildfire Coordinating Group. (2006). *Fireline Handbook, Appendix B: Fire Behavior (PMS 410-1)* (PMS 410-1). National Wildfire Coordinating Group Publications Management System.

North, M. P., Bisbing, S. M., Hankins, D. L., Hessburg, P. F., Hurteau, M. D., Kobziar, L. N., Meyer, M. D., Rhea, A. E., Stephens, S. L., & Stevens-Rumann, C. S. (2024). Strategic fire zones are essential to wildfire risk reduction in the Western United States. *Fire Ecology*, *20*(1), 50, s42408-024-00282-y. https://doi.org/10.1186/s42408-024-00282-y

Palaiologou, P., Giannakopoulos, C., Vasilakos, C., Sakellariou, S., Rodrigues, M., Karali, A., Katavoutas, G., Varotsos, K. V., Roussou, O., Gelabert, P. J., Jiménez-Ruano, A., Lemesios, G., Trasobares, A., Finney, M., & Kalabokidis, K. (2026). A dataset to support wildland fire and fuel management in Greece created with stochastic wildfire simulations. *Data in Brief*, *64*, 112304. https://doi.org/10.1016/j.dib.2025.112304

Parisien, M.-A., Dawe, D. A., Miller, C., Stockdale, C. A., & Armitage, O. B. (2019). Applications of simulation-based burn probability modelling: A review. *International Journal of Wildland Fire*, *28*(12), 913. https://doi.org/10.1071/WF19069

Pausas, JuliG. G., & Fernández-Muñoz, S. (2012). Fire regime changes in the Western Mediterranean Basin: From fuel-limited to drought-driven fire regime. *Climatic Change*, *110*(1-2), 215-226. https://doi.org/10.1007/s10584-011-0060-6

Resco De Dios, V., Cunill Camprubí, À., Campos-Arceiz, A., Clarke, H., He, Y., Zveushe, O. K., Domènech, R., Ying, H., & Yao, Y. (2025). Protected Areas Show Substantial and Increasing Risk of Wildfire Globally. *Fire*, *8*(10), 405. https://doi.org/10.3390/fire8100405

Resco De Dios, V., Schütze, S. J., Cunill Camprubí, À., Balaguer-Romano, R., Boer, M. M., & Fernandes, P. M. (2025). Protected areas as hotspots of wildfire activity in fire-prone Temperate and Mediterranean biomes. *Journal of Environmental Management*, *385*, 125669. https://doi.org/10.1016/j.jenvman.2025.125669

Rich, O., & Ibarra, P. (2015, septiembre). La cartografía de cultivos abandonados y de selección de áreas prioritarias de recuperación como instrumento eficaz del proyecto Banco de tierras de la Comarca del Matarraña. *XXIV Congreso de la Asociación de Geógrafos Españoles*.

Rodrigues, M. (2025, marzo 18). *Introducing SCENFIRE, a Post-Processing of Scenario-Based for the integration of Wildfire simulations*. https://doi.org/10.5194/egusphere-egu25-8974

Rodrigues, M., Alcasena, F., & Vega-García, C. (2019). Modeling initial attack success of wildfire suppression in Catalonia, Spain. *Science of the Total Environment*, *666*, 915-927. https://doi.org/10.1016/j.scitotenv.2019.02.323

Rodrigues, M., Camprubí, À. C., Balaguer-Romano, R., Megía, C. J. C., Castañares, F., Ruffault, J., Fernandes, P. M., & Dios, V. R. de. (2023). Drivers and implications of the extreme 2022 wildfire season in Southwest Europe. *Science of The Total Environment*, *859*, 160320. https://doi.org/10.1016/j.scitotenv.2022.160320

Rodrigues, M., & Gelabert Vadillo, P. J. (2025a). *Future projections of human-caused ignition probability* [Dataset]. Zenodo. https://doi.org/10.5281/ZENODO.17471788

Rodrigues, M., & Gelabert Vadillo, P. J. (2025b). *Future projections of ligthning ignition probability* [Dataset]. Zenodo. https://doi.org/10.5281/ZENODO.17473460

Rodrigues, M., & Gelabert Vadillo, P. J. (2025c). *Future projections of probability of success in the initial attack* [Dataset]. Zenodo. https://doi.org/10.5281/ZENODO.17473051

Rodrigues, M., Jiménez-Ruano, A., Gelabert, P. J., de Dios, V. R., Torres, L., Ribalaygua, J., & Vega-García, C. (2023). Modelling the daily probability of lightning-caused ignition in the Iberian Peninsula. *International Journal of Wildland Fire*. https://doi.org/10.1071/WF22123

Salis, M., Del Giudice, L., Arca, B., Ager, A. A., Alcasena-urdiroz, F., Lozano, O., Bacciu, V., & Spano, D. (2018). Modeling the effects of different fuel treatment mosaics on wild fi re spread and behavior in a Mediterranean agro-pastoral area. *Journal of Environmental Management*, *212*, 490-505. https://doi.org/10.1016/j.jenvman.2018.02.020

Salis, M., Del Giudice, L., Jahdi, R., Alcasena-Urdiroz, F., Scarpa, C., Pellizzaro, G., Bacciu, V., Schirru, M., Ventura, A., Casula, M., Pedes, F., Canu, A., Duce, P., & Arca, B. (2022). Spatial Patterns and Intensity of Land Abandonment Drive Wildfire Hazard and Likelihood in Mediterranean Agropastoral Areas. *Land*, *11*(11), 1942. https://doi.org/10.3390/land11111942

San-Miguel-Ayanz, J., Schulte, E., Schmuck, G., Camia, A., Strobl, P., Liberta, G., Giovando, C., Boca, R., Sedano, F., Kempeneers, P., McInerney, D., Withmore, C., Santos de Oliveira, S., Rodrigues, M., Durrant, T., Corti, P., Oehler, F., Vilar, L., & Amatulli, G. (2012). Comprehensive monitoring of wildfires in europe: The European Forest Fire Information System (EFFIS). En J. Tiefenbacher (Ed.), *Approaches to Managing Disaster—Assessing Hazards, Emergencies and Disaster Impacts* (pp. 87-105). InTech.

Schulp, C. J. E., Levers, C., Kuemmerle, T., Tieskens, K. F., & Verburg, P. H. (2019). Mapping and modelling past and future land use change in Europe's cultural landscapes. *Land Use Policy*, *80*, 332-344. https://doi.org/10.1016/j.landusepol.2018.04.030

Scott, J. H., & Burgan, R. E. (2005). Standard Fire Behavior Fuel Surface Fire Spread Model Set for Use with Rothermel's Models: A Comprehensive. En *Department of Agriculture, Forest Service* (June; Vol. 76, p. 72 p.). https://doi.org/10.1016/j.jfluidstructs.2017.11.007

Seidl, R., Fernandes, P. M., Fonseca, T. F., Gillet, F., Jönsson, A. M., Merganičová, K., Netherer, S., Arpaci, A., Bontemps, J.-D., Bugmann, H., González-Olabarria, J. R., Lasch, P., Meredieu, C., Moreira, F., Schelhaas, M.-J., & Mohren, F. (2011). Modelling natural disturbances in forest ecosystems: A review. *Ecological Modelling*, *222*(4), 903-924. http://dx.doi.org/10.1016/j.ecolmodel.2010.09.040

Seidl, R., Thom, D., Kautz, M., Martin-Benito, D., Peltoniemi, M., Vacchiano, G., Wild, J., Ascoli, D., Petr, M., Honkaniemi, J., Lexer, M. J., Trotsiuk, V., Mairota, P., Svoboda, M., Fabrika, M., Nagel, T. A., & Reyer, C. P. O. (2017). Forest disturbances under climate change. *Nature Climate Change*, *7*(6), 395-402. https://doi.org/10.1038/nclimate3303

Seijo, F., & Gray, R. (2012). Pre-Industrial Anthropogenic Fire Regimes in Transition: The Case of Spain and its Implications for Fire Governance in Mediterranean Type Biomes. *Human Ecology Review*, *19*(1), 58-69.

Sil, Â., Azevedo, J. C., Fernandes, P. M., & Honrado, J. P. (2024). Will fire-smart landscape management buffer the effects of climate and land-use changes on fire regimes? *Ecological Processes*, *13*(1), 57. https://doi.org/10.1186/s13717-024-00535-3

Simon, B., Crowley, C., & Franco, F. (2022). The Costs and Costs Avoided From Wildfire Fire Management—A Conceptual Framework for a Value of

Information Analysis. *Frontiers in Environmental Science*, *10*, 804958. https://doi.org/10.3389/fenvs.2022.804958

Stougiannidou, D., & Zafeiriou, E. (2022). Wildfire economic impact assessment: An empirical model-based investigation for Greek agriculture. *Modeling Earth Systems and Environment*, *8*(3), 3357-3371. https://doi.org/10.1007/s40808-021-01306-1

Ursino, N., & Romano, N. (2014). Wild forest fire regime following land abandonment in the Mediterranean region. *Geophysical Research Letters*, *41*(23), 8359-8368. https://doi.org/10.1002/2014GL061560

Vidal-Macua, J. J., Ninyerola, M., Zabala, A., Domingo-Marimon, C., Gonzalez-Guerrero, O., & Pons, X. (2018). Environmental and socioeconomic factors of abandonment of rainfed and irrigated crops in northeast Spain. *Applied Geography*, *90*(September 2017), 155-174. https://doi.org/10.1016/j.apgeog.2017.12.005

Viedma, O., Moity, N., & Moreno, J. M. (2015). Changes in landscape fire-hazard during the second half of the 20th century: Agriculture abandonment and the changing role of driving factors. *Agriculture, Ecosystems & Environment*, *207*, 126-140. https://doi.org/10.1016/j.agee.2015.04.011

Wunder, S., Calkin, D. E., Charlton, V., Feder, S., Martínez de Arano, I., Moore, P., Rodríguez y Silva, F., Tacconi, L., & Vega-García, C. (2021). Resilient landscapes to prevent catastrophic forest fires: Socioeconomic insights towards a new paradigm. *Forest Policy and Economics*, *128*, 102458. https://doi.org/10.1016/j.forpol.2021.102458

Table S1. Summary of weather type conditions used in wildfire spread simulation. WT stands for the dominant weather types observed in the region obtained by using a K-means cluster procedure from historical wildfires (min k=4); WS is the 95th percentile of wind speed (km h^{-1}); RH is the 5th percentile of relative humidity (%); T is the 95th percentile of temperature (ºC); Freq. WT is the relative frequency of observation of the WT; WD is the dominant wind direction; Freq. WD is the relative frequency of WD within the WT; BA is the observed burned area (ha) in the WD and WT; and Freq. Simulation is the proportion of burned area across all WT and WD.

WT	WS	RH	T	Freq. WT	WD	Freq. WD	BA	Freq. Simulation
					N	0.02	11.7	0.01
					NE	0.00		0.00
					E	0.09	73.5	0.04
1	28.94	21.89	34.73	0.43	SE	0.60	1112.4	0.26
					S	0.09	509.2	0.04
					SW	0.00		0.00

					W	0.06	4.2	0.02
					NW	0.13	26.5	0.06
2	37.55	27.96	25.73	0.23	N	0.00		0.00
					NE	0.00		0.00
					E	0.00		0.00
					SE	0.29	85.8	0.07
					S	0.07	6.5	0.02
					SW	0.00		0.00
					W	0.07	4.1	0.02
					NW	0.57	46.0	0.13
3	24.78	49.46	23.55	0.11	N	0.31	4.9	0.03
					NE	0.00		0.00
					E	0.08	3.0	0.01
					SE	0.46	28.0	0.05
					S	0.00		0.00
					SW	0.08	1.0	0.01
					W	0.00		0.00
					NW	0.08	1.0	0.01
4	21.67	25.57	26.45	0.24	N	0.03	1.3	0.01
					NE	0.03	2.5	0.01
					E	0.14	14.1	0.03
					SE	0.31	41.5	0.07
					S	0.07	28.0	0.02
					SW	0.03	1.0	0.01
					W	0.07	5.4	0.02
					NW	0.31	30.3	0.07

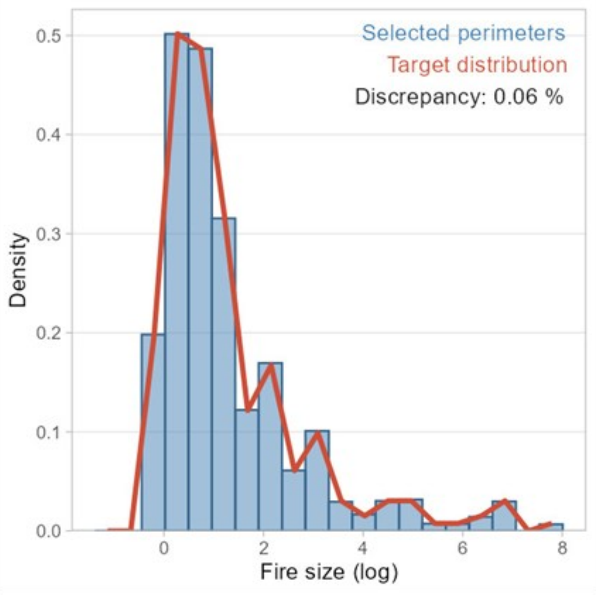

Figure S1. Historical fire size density distribution in the Matarranya region (red line) and frequency histogram of the 20,000 simulated fires. The discrepancy value indicates the percent difference between the historical and simulated fire size distribution.

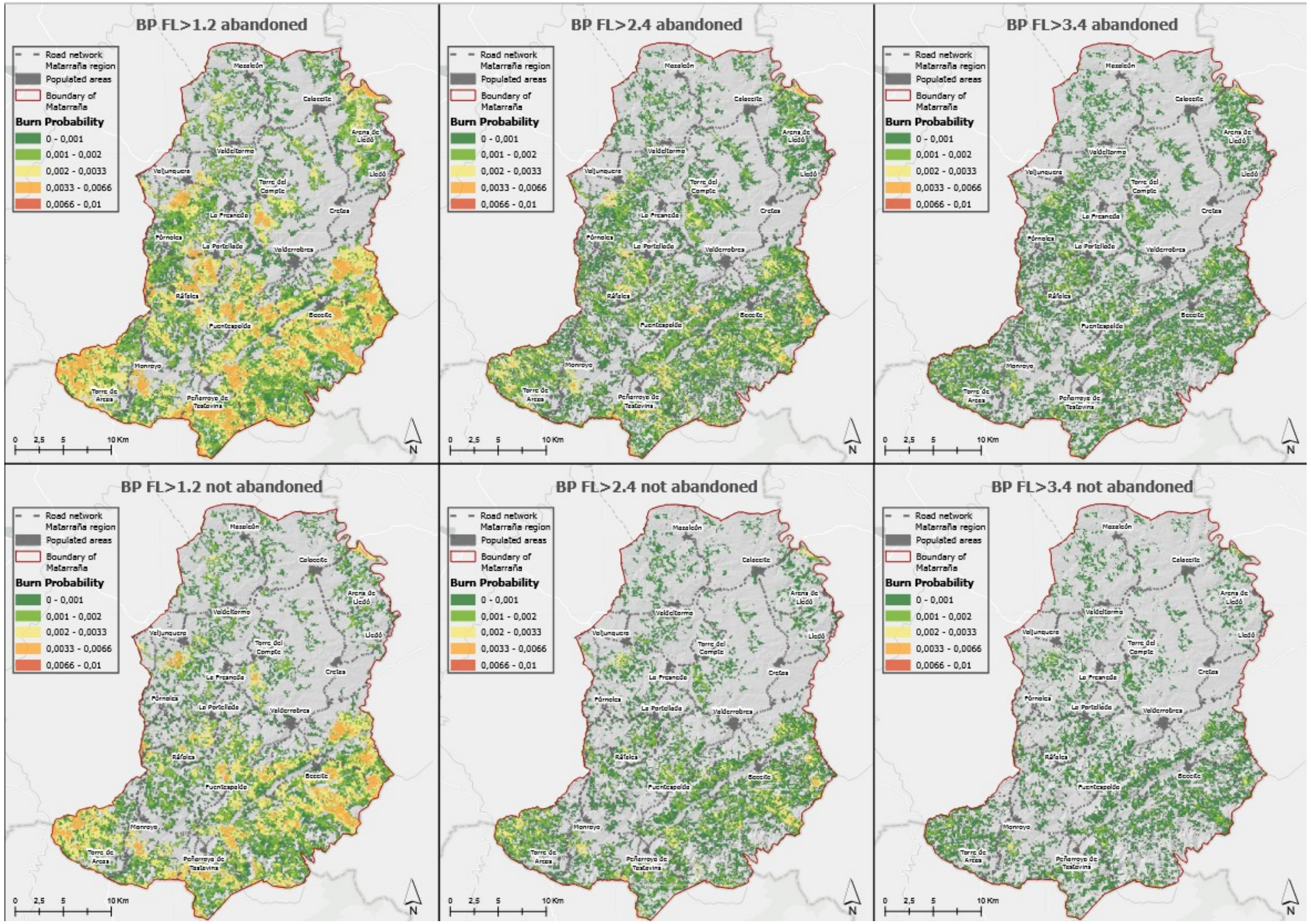

Figure S2. Spatial distribution of BPa across the Matarranya region under two land-use scenarios: (bottom) no-abandonment (NO-AB), (top) abandonment (AB). Burn probability classes were expressed as return intervals (RI) with breakpoints at 0.0010, 0.0020, 0.0033, 0.0066 BPa, corresponding to 1000, 500, 300 and 150 years. Maps represent increasing thresholds of flame length from left to right.

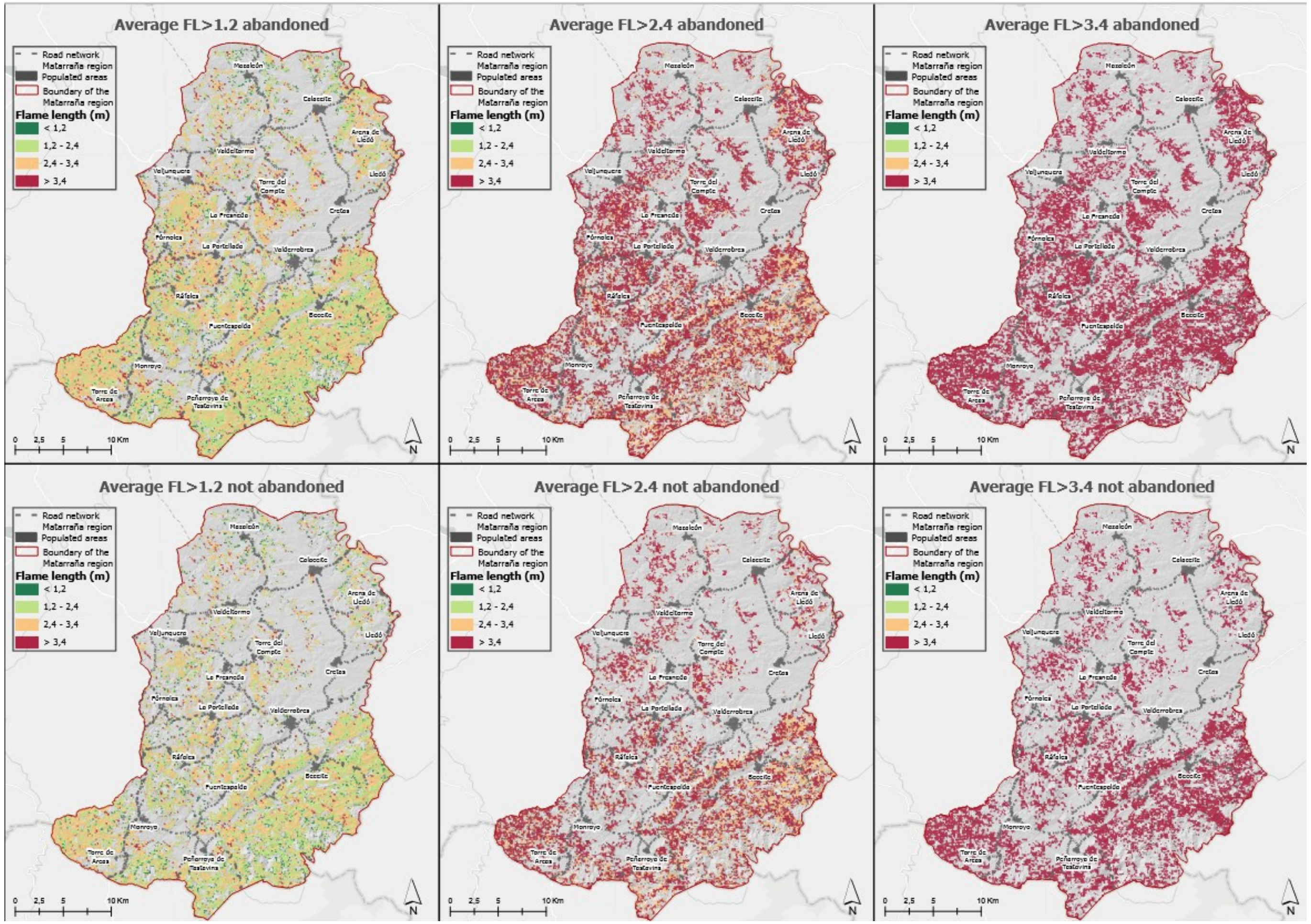

Figure S3. Spatial distribution of flame length (m) across the Matarranya region under two land-use scenarios: (bottom) no-abandonment (NO-AB), (top) abandonment (AB).

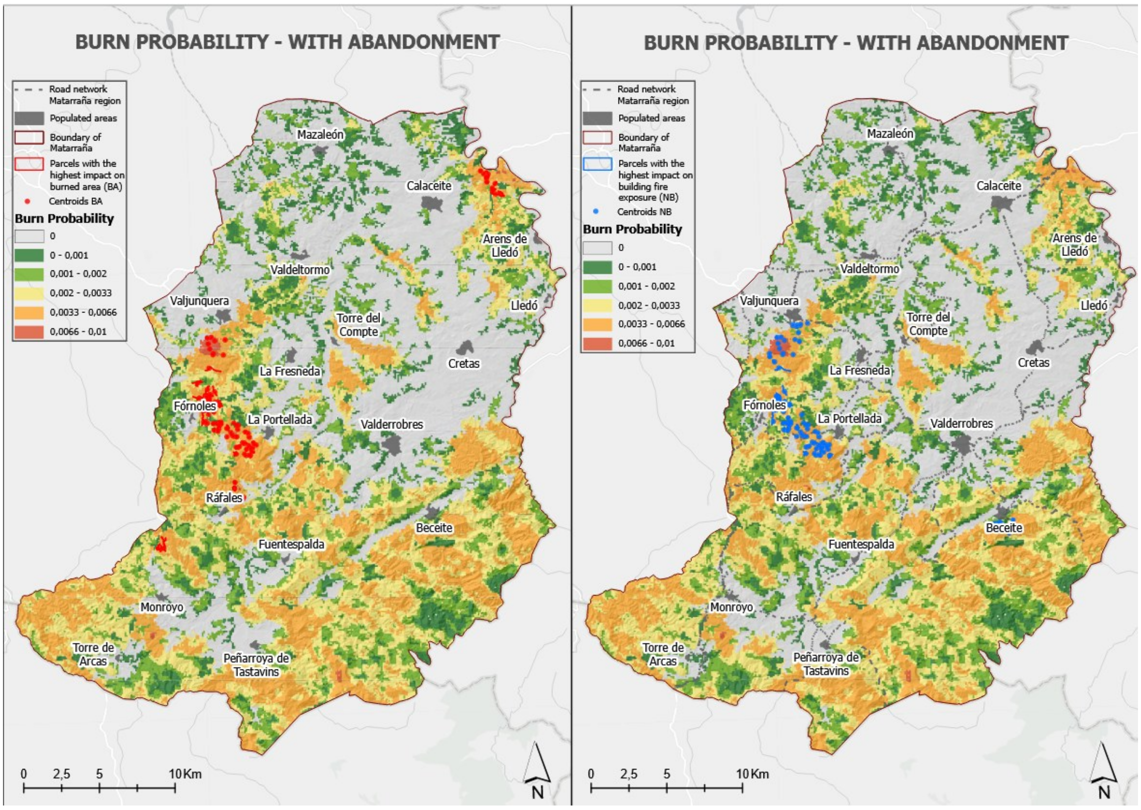

Figure S4. Location of the top 100 most influential plots in terms of size of simulated fires (left) and number of buildings inside simulated fire scars (right). Color maps represent BPa in the abandonment baseline.